



## Original article

## Design, synthesis and X-ray crystallographic study of NAMPRase inhibitors as anti-cancer agents

Hyun You<sup>b,1</sup>, Hyung-Seop Youn<sup>a,1</sup>, Isak Im<sup>a,1</sup>, Man-Ho Bae<sup>a</sup>, Sang-Kook Lee<sup>c</sup>, Hyojin Ko<sup>b,\*\*</sup>, Soo Hyun Eom<sup>a,\*\*</sup>, Yong-Chul Kim<sup>a,b,\*</sup><sup>a</sup> School of Life Science, Gwangju Institute of Science and Technology, Gwangju 500-712, Republic of Korea<sup>b</sup> Graduate-program of Medical System Engineering (GMSE), Gwangju Institute of Science and Technology, Gwangju 500-712, Republic of Korea<sup>c</sup> College of Pharmacy, Seoul National University, Seoul 151-742, Republic of Korea

## ARTICLE INFO

## Article history:

Received 1 September 2010

Received in revised form

4 January 2011

Accepted 12 January 2011

Available online 31 January 2011

## Keywords:

Nicotinamide phosphoribosyltransferase (NAMPRase)

Pre-B-cell colony-enhancing factor (PBEF)

FK866

Nicotinamide adenine dinucleotide (NAD<sup>+</sup>)

X-ray crystal structure

## ABSTRACT

NAMPRase (PBEF/Visfatin) plays a pivotal role in the salvage pathway of NAD<sup>+</sup> biosynthesis. NAMPRase has been an attractive target for anti-cancer agents that induce apoptosis of tumor cells via a declining plasma NAD<sup>+</sup> level. In this report, a series of structural analogs of FK866 (**1**), a known NAMPRase inhibitor, was synthesized and tested for inhibitory activities against the proliferation of cancer cells and human NAMPRase. Among them, compound **7** showed similar anti-cancer and enzyme inhibitory activities to compound **1**. Further investigation of compound **7** with X-ray analysis revealed a co-crystal structure in complex with human NAMPRase, suggesting that Asp219 in the active site of the enzyme could contribute to an additional interaction with the pyrrole nitrogen of compound **7**.

© 2011 Elsevier Masson SAS. All rights reserved.

## 1. Introduction

Nicotinamide adenine dinucleotide (NAD<sup>+</sup>) is generally considered a key component involved in redox reactions, and it plays various remarkable roles in a range of NAD<sup>+</sup>-dependent biological processes including signal transduction, DNA repair, and post-translational protein modification [1]. It has been revealed that NAD<sup>+</sup> is a substrate for poly (ADP-ribose) polymerase (PARP) and a specific subclass of histone deacetylases that are known as sirtuins [2], which are involved in genomic stability, apoptosis, aging, stress resistance, and metabolism [3–6]. Since most cancer cells have continuous PARP activation through DNA damage and genomic instability [7–10] and they have higher energy consumption demands relative to non-transformed cells [11], cancer cells are expected to be more vulnerable to the inhibition of NAD<sup>+</sup> synthesis than non-transformed cells. Nicotinamide

phosphoribosyltransferase (NAMPRase) is also known as pre-B-cell colony-enhancing factor 1 (PBEF) or visfatin, and it is the rate-limiting enzyme for nicotinamide adenine dinucleotide (NAD<sup>+</sup>) biosynthesis from nicotinamide. Indeed, NAMPRase over-expression was shown to maintain adequate levels of NAD<sup>+</sup> in cancer cells [12,13]. Eukaryotic cells possess several mechanisms to replenish NAD including a *de novo* synthesis pathway from the amino acid tryptophan, and there are at least two salvage/recycling pathways [14,15]. One of these pathways relies on the enzyme NAMPRase that converts nicotinamide into nicotinamide mononucleotide (NMN), which is subsequently converted to NAD<sup>+</sup> by NMN adenylyltransferase (NMNAT).

A novel antitumor agent FK866 (**1**, Fig. 1) was reported to induce apoptosis of tumor cells by reducing the steady state intracellular NAD<sup>+</sup> levels, and this process was mediated through specific inhibition of NAMPRase [16]. Indeed, inhibition of this enzyme alone appears to have an important impact on NAD<sup>+</sup> levels in a number of cell types. Thus, the enzymes involved in NAD<sup>+</sup> metabolism have become attractive targets for cancer therapy [17]. FK866 has successfully completed a Phase I study, and it is currently being investigated in Phase I/II and II trials for the treatment of various cancers [18]. Recent reports have shown some obstacles to utilize FK866 as an anti-cancer agent: the rapid intravenous

\* Corresponding author. Graduate-program of Medical System Engineering (GMSE), Gwangju Institute of Science and Technology, Gwangju 500-712, Republic of Korea. Tel.: +82 62 970 2502; fax: +82 62 970 2484.

\*\* Corresponding authors.

E-mail address: [yongchul@gist.ac.kr](mailto:yongchul@gist.ac.kr) (Y.-C. Kim).

<sup>1</sup> These authors equally contributed to the work.

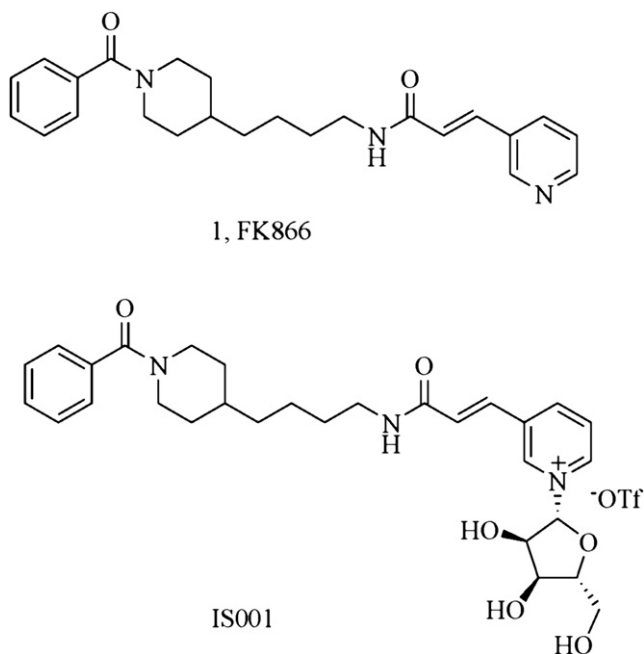


Fig. 1. Structure of FK866 and IS001.

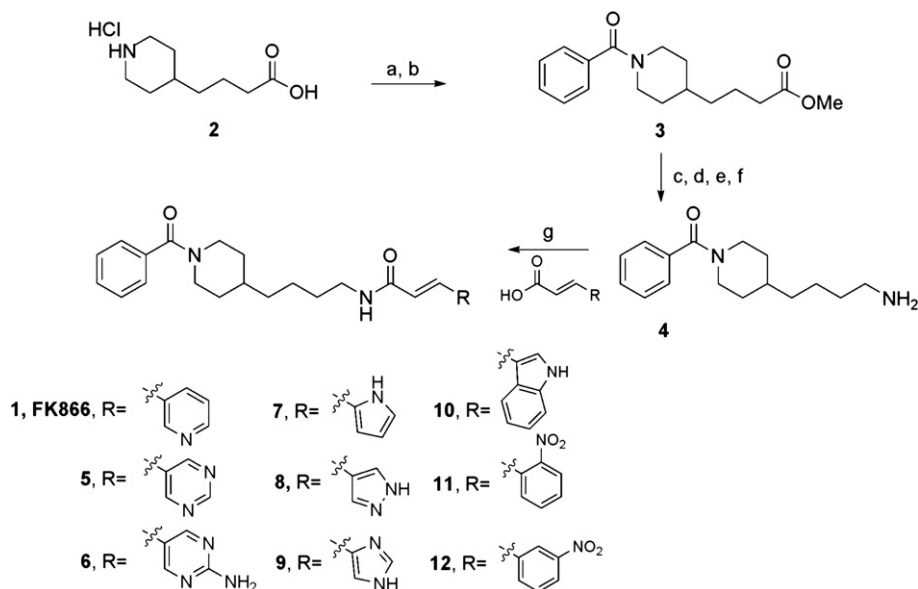
clearance of FK866 through the metabolite FK866-*N*-oxide *in vivo* and the dose limit toxicity due to thrombocytopenia. The crystal structure of NAMPRase with FK866 showed that FK866 is bound in a tunnel at the interface of the NAMPRase dimer through primarily hydrophobic interactions [19,20]. This long (15 Å) and narrow diameter (6 Å) tunnel ends at the active site where the natural substrate nicotinamide (NM) binds by  $\pi$ - $\pi$ -stacking interactions with Phe193 and Tyr18'. In contrast, nicotinamide mononucleotide (NMN), which is the product of the enzyme reaction, is involved in a network of many hydrogen bonds via the ribose ring, and the phosphate group is surrounded by a highly hydrophilic active site.

Due to the long, narrow binding pocket of FK866, modification of FK866 appears to be limited to each end portion. The metabolite FK866-*N*-oxide is the primary problem of FK866; thus, further modification of the pyridine residue of FK866 has been suggested. We previously investigated an FK866 analog, IS001 (Fig. 1), which has an additional ribose ring at the nitrogen of the pyridine ring, using co-crystal structure with NAMPRase [21]. Although IS001 had an almost identical binding mode to that of FK866, the binding affinity of IS001 is dramatically decreased [21]. The X-ray co-crystal structure of IS001 with NAMPRase showed that the additional ribose ring did not have any strong interaction with the hydrophilic residues of NAMPRase. The additional ribose ring possibly interferes with the most stable conformation of the FK866 moiety because of the relatively bulky constrained structure that is connected to the pyridine nitrogen. Herein, we have investigated the design and synthesis of FK866 analogs by combining FK866 and a ribose-mimicking moiety to reduce the constraints of the ribose ring, expecting a tighter interaction by the additional hydrogen bonds. We also replaced the pyridine ring of FK866 with various heteroaromatic rings for combination with a simple ribose-mimicking moiety containing a diol group. The mode of binding and biological activity was assessed by X-ray crystal structure and cell- and enzyme-based assay.

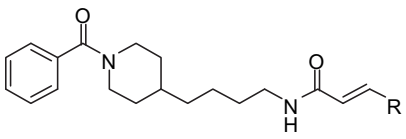
## 2. Results and discussion

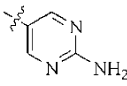
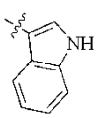
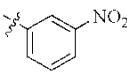
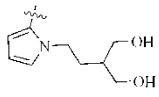
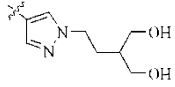
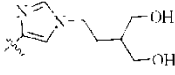
### 2.1. Chemistry

The general synthetic method for the FK866 analogs is described in Scheme 1. The commercially available 4-piperidine butyric acid hydrochloride (**2**) was esterified by treatment with thionyl chloride in methanol; then, it was benzoylated using benzoyl chloride to produce compound **3**. The *N*-benzoated ester (**3**) was reduced to an alcohol by LAH and subsequently transformed into an amine (**4**) by two step reactions with potassium phthalimide and hydrazine hydrate. Compound **4** was subjected to coupling reactions with several heteroaromatic acrylic acids, such as pyrimidine, aminopyrimidine, pyrrole, pyrazole groups, urocanic acid, trans-3-indole acrylic acids, and nitrocinnamic acids to produce FK866 analogs

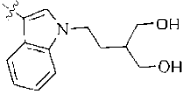
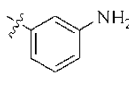


Scheme 1. Synthesis of FK866 analogs 1. (a)  $\text{SOCl}_2$ , MeOH, RT, 2 h, 89%; (b) benzyl chloride, pyridine, DCM, RT, 3 h, 68%; (c) LAH, THF, RT, 2 h, 65%; (d) methanesulfonyl chloride, TEA, DCM, RT, 2 h, 68%; (e) potassium phthalimide, DMF, 50 °C, 8 h, 87%; (f) hydrazine hydrate, EtOH, RT, 1 day, 52%; (g) EDC, HOBt, TEA, DCM or DMF, RT, 3–4 h, 70%.

**Table 1**  
Effects of FK866 (**1**) and its analogs **5–12**, **14–20** on MCF7 cell viability.


Compounds (10 $\mu$ M)	R	Cell Viability MCF7 <sup>a</sup> (% of control)	IC <sub>50</sub> ( $\mu$ M)
<b>1</b> , FK866		5.6 $\pm$ 0.5	0.68 $\pm$ 0.1
<b>5</b>		86.8 $\pm$ 2.6	
<b>6</b>		103.4 $\pm$ 0.7	
<b>7</b>		4.5 $\pm$ 0.8	1.29 $\pm$ 0.05
<b>8</b>		101.7 $\pm$ 2.4	
<b>9</b>		102.9 $\pm$ 0.7	
<b>10</b>		103.3 $\pm$ 0.5	
<b>11</b>		102.7 $\pm$ 0.2	
<b>12</b>		103.1 $\pm$ 0.4	
<b>14</b>		105.0 $\pm$ 0.7	
<b>15</b>		106.6 $\pm$ 1.2	
<b>16</b>		104.3 $\pm$ 0.9	

**Table 1** (continued).

Compounds (10 $\mu$ M)	R	Cell Viability MCF7 <sup>a</sup> (% of control)	IC <sub>50</sub> ( $\mu$ M)
<b>17</b>		104.9 $\pm$ 1.1	
<b>18</b>		103.6 $\pm$ 0.4	
<b>19</b>		106.3 $\pm$ 1.5	
<b>20</b>		103.9 $\pm$ 0.5	

<sup>a</sup> Values are given by the means of three experiments with standard deviations.

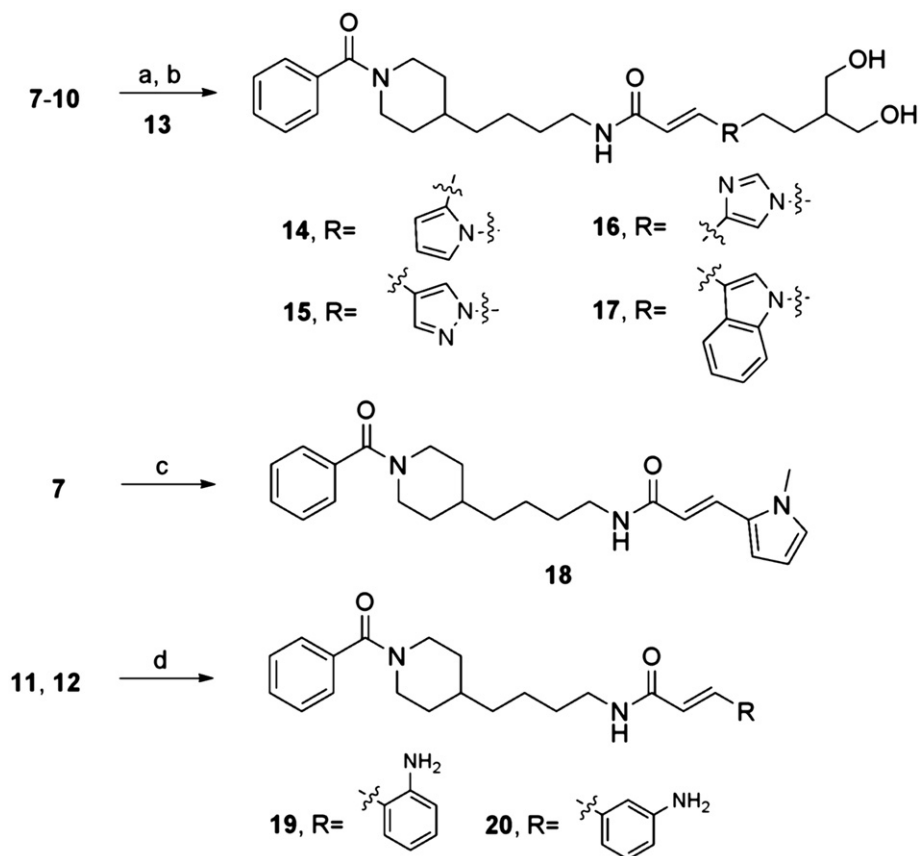
(**5–12**) (Scheme 1 and Table 1). Compounds **7–10** were further *N*-alkylated with **13** followed by deprotections of the acetonide group to afford compounds **14–17** containing ribose-mimicking 2-ethylpropane-1,3-diol moieties. Compound **18** was prepared from a methylation reaction of **7**, and compound **19** and **20** were obtained by reductions of the nitro groups of **11** and **12**, respectively (Scheme 2 and Table 1).

Scheme 3 shows the preparation of the heteroaromatic acrylic acids as building blocks. 5-bromo-pyrimidine (**21a**), 5-bromopyrimidin-2-amine (**21b**), Boc-pyrrole (**26**) and tosylated 4-bromo pyrazole (**30**) were reacted with methyl acrylate (**22**) under microwave-assisted Heck reaction conditions, and followed by deprotection and hydrolysis reactions to yield each acrylic acid (**23**, **24**, **28**, and **31**). Other heteroaromatic acrylic acids used in this study were purchased from commercial resources.

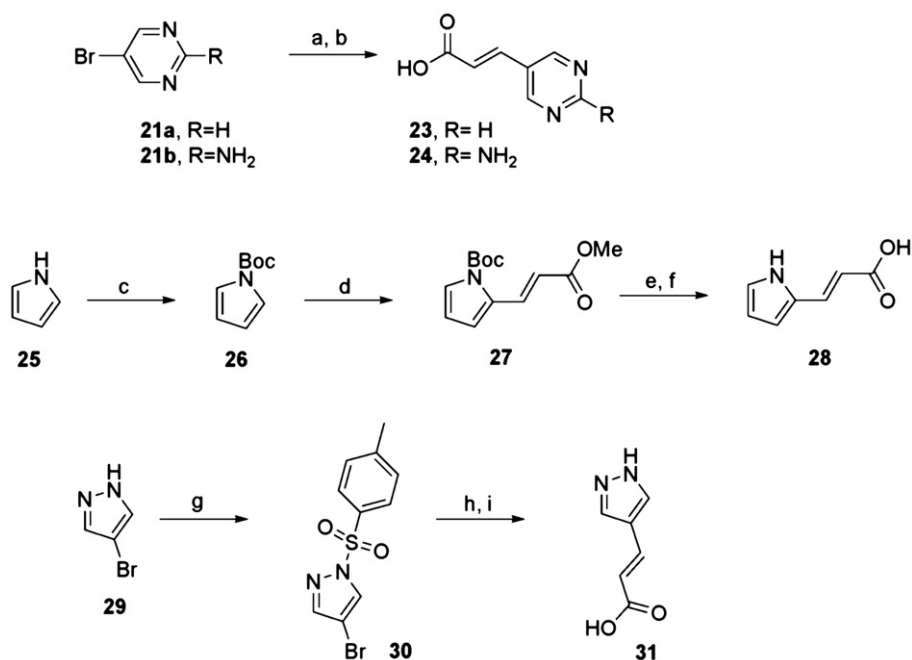
The 2-ethylpropane-1,3-diol analog (**13**) was prepared from decarboxylation of triethyl-1,1,2-ethane tricarboxylate (**32**) followed by a protection reaction of the diol group of **33** with 2,3-dimethoxy propane (Scheme 4).

## 2.2. Cell viability assay

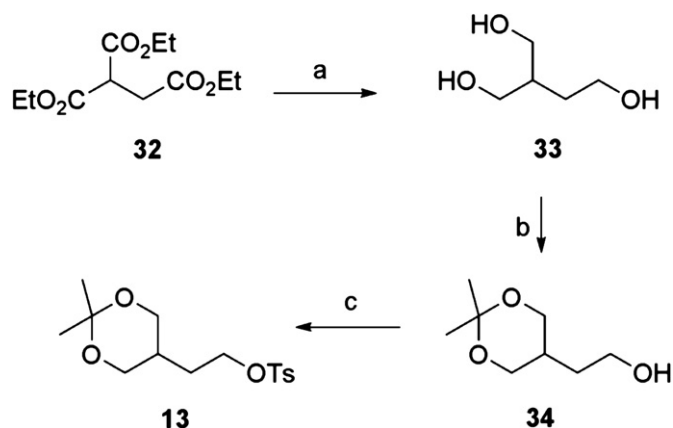
A cell viability assay was conducted to test the synthesized FK866 analogs [15] on MCF7 breast cancer cells. Briefly, the cells were incubated for six days with a fixed concentration of the compounds, and the viability was measured by an SRB assay. The induction of delayed cell death of the tumor cells appeared prominent after six days of FK866 treatment on the SRB assay. The structure and activity of the FK866 analogs are shown in Table 1. Substitution of the pyridine ring of FK866 with various heteroaromatic rings (**5–10**) revealed a great loss of anti-cancer activity except for compound **7** with the pyrrole group. Even a one-point substitution, such as carbon for nitrogen at the pyridine ring (**5**), dramatically dropped the activity. However, compound **7** maintained an activity similar to that of FK866 at 10  $\mu$ M. Although the addition of a ribose-mimicking diol moiety in the structure (**7** to **14**) would theoretically improve the activity, compound **14** turned out to be inactive. Also, the compounds with a ribose-mimicking diol moiety on the other heteroaromatic rings (**15–17**) failed to inhibit



**Scheme 2.** Synthesis of FK866 analogs II. (a) NaH, DMF, RT, 10 h; (b) 1 N HCl, THF, RT, 2 h; (c) NaH, CH<sub>3</sub>I, DMF, 55 °C, 9 h; (d) SnCl<sub>2</sub>, EtOH, 70 °C, 1.2 h.



**Scheme 3.** Synthesis of acrylic acid building blocks. (a) methyl acrylate, TEA, Pd(OAc)<sub>2</sub>, acetonitrile, 170 °C, 20 min, microwave, 27%; (b) 5% NaOH, MeOH : Water = (4:1), RT, 2 h, 70%; (c) Boc<sub>2</sub>O, TEA, DCM, RT, 2 h, 94%; (d) methyl acrylate, Pd(OAc)<sub>2</sub>, acetic acid-dioxane-DMF (3:9:1), RT, 96 h, 23%; (e) TFA-CH<sub>2</sub>Cl<sub>2</sub> (3:10), 1 h, 75%; (f) 5% NaOH, MeOH–Water (4:1), 4 h, 91%; (g) *p*-toluene sulfonyl chloride, TEA, DCM, RT, 3 h, 73%; (h) methyl acrylate, TEA, Pd(OAc)<sub>2</sub>, LiCl, *p*(*o*-tol)<sub>3</sub>, DMF, 140 °C, overnight, 38%; (i) 5% NaOH, MeOH–Water (4:1), 4 h, 78%.



**Scheme 4.** Preparation of ribose mimic moiety. (a)  $\text{NaBH}_4$ , MeOH, tert-butyl alcohol, reflux, 1 h, 88%; (b) 2,2-dimethoxy propane, *p*-toluene sulfonic acid, THF, RT, 4 h, 59%; (c) *p*-toluene sulfonyl chloride, pyridine, DCM, RT, 5 h, 58%.

cell viability. Therefore, even a relatively small ribose-mimicking diol moiety in **14**–**17** seems to interfere with the interaction with the enzyme (i.e. the ribose moiety in IS001).

Moreover, compound **18** with *N*-methylation at the pyrrole group of **7** showed significant loss of the activity, suggesting the hydrogen of the pyrrole group is important. Compounds **11**, **12**, **19**, and **20**, which had nitro or aminophenyl moieties instead of heterocycles, did not improve the cytotoxic activity, indicating that the interaction of the pyridine moiety of FK866 with the corresponding binding region of the enzyme must be tightly managed for attempted modifications.

We then compared FK866 and compound **7** via the concentration-response curves of both compounds. The  $\text{IC}_{50}$  values of FK866 and compound **7** demonstrating their cytotoxicity against MCF7 cells were determined as 0.68  $\mu\text{M}$  and 1.29  $\mu\text{M}$ , respectively, indicating that compound **7** might be another possible candidate as an anti-cancer agent (Fig. 2). Therefore, the anti-cancer activities of compound **7** and FK866 were investigated for five other cancer cell lines (Table 2). The effect of compound **7** in the other cancer cells was consistent with that on the MCF7 cells in the low micromolar range of  $\text{IC}_{50}$  values, whereas FK866 generally showed higher activity with submicromolar range of  $\text{IC}_{50}$  values. However, compound **7** showed superior anti-cancer activity to

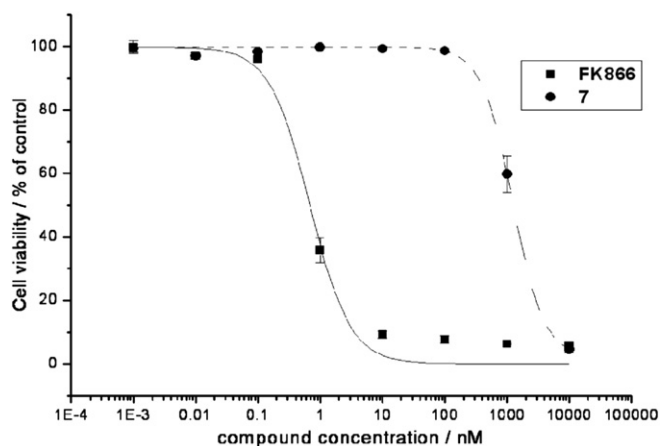


**Fig. 2.** MCF7 cell viability after 6 day in the presence of increasing concentrations of compounds FK866 and **7**.

FK866 ( $\text{IC}_{50} > 20 \mu\text{M}$ ) in human leukemia cells (K562) with an  $\text{IC}_{50}$  value of 1.4  $\mu\text{M}$ .

### 2.3. Enzyme assay using HPLC

We performed an *in vitro* enzyme assay using an HPLC system to evaluate the inhibitory activity of FK866 and compound **7**. In the presence of FK866, the formation of NMN as a NAMPrTase reaction product from two reactants (NM and PRPP) was significantly decreased in HPLC analysis by monitoring the UV absorbance at 261 nm (Fig. 3). In our data, two compounds showed similar *in vitro* enzyme inhibitory activities, which was consistent to the cell-based anti-proliferative activities. The  $\text{IC}_{50}$  values obtained from the concentration-dependent inhibition curves of FK866 and compound **7** showed comparable values, 14.8 and 20.3  $\mu\text{M}$ , respectively (Fig. 4).

### 2.4. Crystal structure

The crystal structure of human NAMPrTase in complex with compound **7** showed a dimer in crystal packing and 1:1 stoichiometry (Fig. 5), and this is consistent with the previously reported data of the human NAMPrTase-FK866 complex assessed using gel filtration and dynamic light scattering [19]. Moreover, the binding site of **7** was nearly identical to that of FK866 and NMN, which are the active sites of NAMPrTase formed around the dimeric interface (Fig. 6). The binding sites of both inhibitors, except the pyridine or pyrrole ring, into NAMPrTase consisted of primarily hydrophobic interactions at Val242(A), Ala244(A), Ile309(A), Arg349(A), Val350(A), Ile351(A), Ala379(A), and Asp16(B). In addition, the pyrrole ring made  $\pi$ - $\pi$  stacking interactions with Phe193(A) and Tyr18(B) identical to that on the pyridine ring of FK866. The hydrophobic bond length between Asp16(B) of NAMPrTase and the pyrrole ring of FK866 (4.09 Å) was slightly closer than that of the pyrrole ring of **7** (4.53 Å). Interestingly, Asp219(A) interacted with the NAMPrTase-**7** complex through additional ionic interaction with the pyrrole ring; however, this residue showed no interaction with the pyridine ring of FK866, as shown in Fig. 7. This interaction might contribute to the structural stabilization between NAMPrTase and **7**, or we propose that the pyridine ring of FK866 may rotate allowing it to make the ionic interaction with Asp219(A) of human NAMPrTase in the complex of FK866 (PDB code 2GVJ). In addition, although we did not determine the structures of NAMPrTase in complex with the other candidates, the results of the cell viability assays suggest that the addition of a bulky or hydrophilic moiety cannot improve the interaction with NAMPrTase due to the steric hindrance and the destabilized hydrophobic interactions. It might be further explained by the binding mode of FK866, which has a hydrogen bond with Asp219 through a water molecule in the 'tunnel'. This entropically disadvantageous interaction can be altered easily by small molecular changes derived from the modification of FK866. If the optimal binding interactions of the pyridine

**Table 2**  
 $\text{IC}_{50}$  ( $\mu\text{M}$ ) cytotoxicity on various cancer cell lines.

	K562 <sup>a</sup>	SNU638 <sup>b</sup>	HT1080 <sup>c</sup>	A549 <sup>d</sup>	HCT116 <sup>e</sup>
FK866	>20	<0.16	<0.16	<0.16	<0.16
<b>7</b>	1.40	1.70	3.20	4.86	0.30
Ellipticine	0.38	1.64	0.21	0.47	0.41

<sup>a</sup> K562 : human leukemia cell.

<sup>b</sup> SNU638 : human stomach cancer cell.

<sup>c</sup> HT1080 : human sarcoma cell.

<sup>d</sup> A549 : human lung cancer cell.

<sup>e</sup> HCT116 : human colon cancer cell.

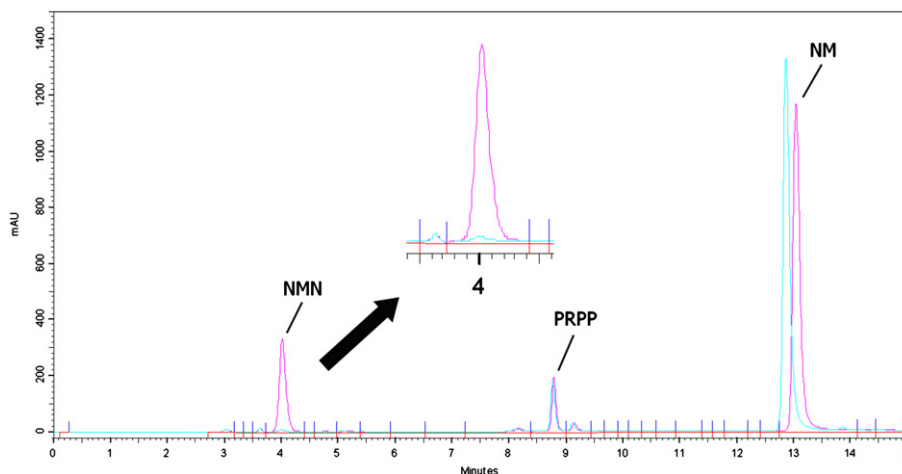


**Fig. 3.** The products of human NAMPTase reaction were analyzed by HPLC. Elution times for each chemical were confirmed by running standards in the same HPLC conditions. The products of reaction without FK866 were shown in pink, and the products with 100  $\mu\text{M}$  FK866 were shown in cyan. (For interpretation of the references to color in this figure legend, the reader is referred to the web version of this article.)

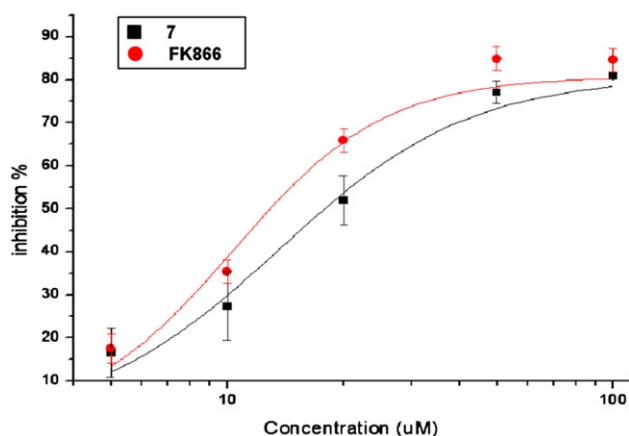


**Fig. 4.** 5, 10, 20, 50, and 100  $\mu\text{M}$  FK866 and 7 were added to reaction buffer, respectively. All experiments were triplicated, error bars represent standard deviation.

ring moiety through  $\pi$ - $\pi$ -stacking interactions (Phe193, Tyr18') are not conserved, then the hydrogen bonds with Asp219 via a water molecule might be disturbed by slight delocalization of the pyridine ring moiety. In which case, an FK866 analog is not strong enough to compete with a natural substrate since the other part of the analog is far from the active site and it has no significant interactions to hold the whole inhibitor inside the binding tunnel.

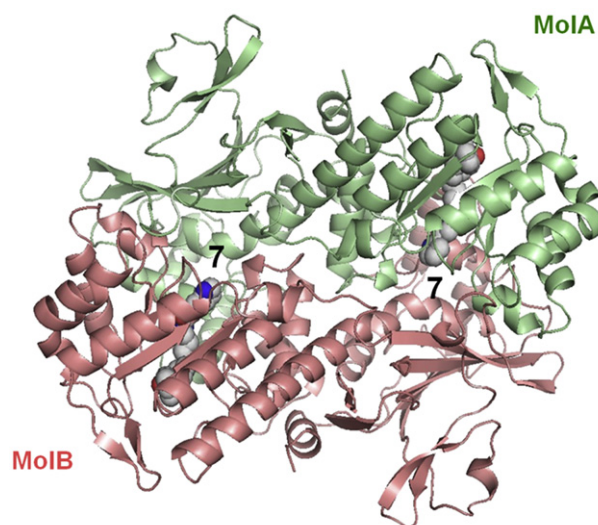


**Fig. 5.** Schematic representation of the NAMPTase-7 complex. In ribbon diagram of NAMPTase dimer, two NAMPTase monomers were shown in green (MoIA) and pink (MoIB), respectively. 7 were displayed as sphere models. (For interpretation of the references to color in this figure legend, the reader is referred to the web version of this article.)

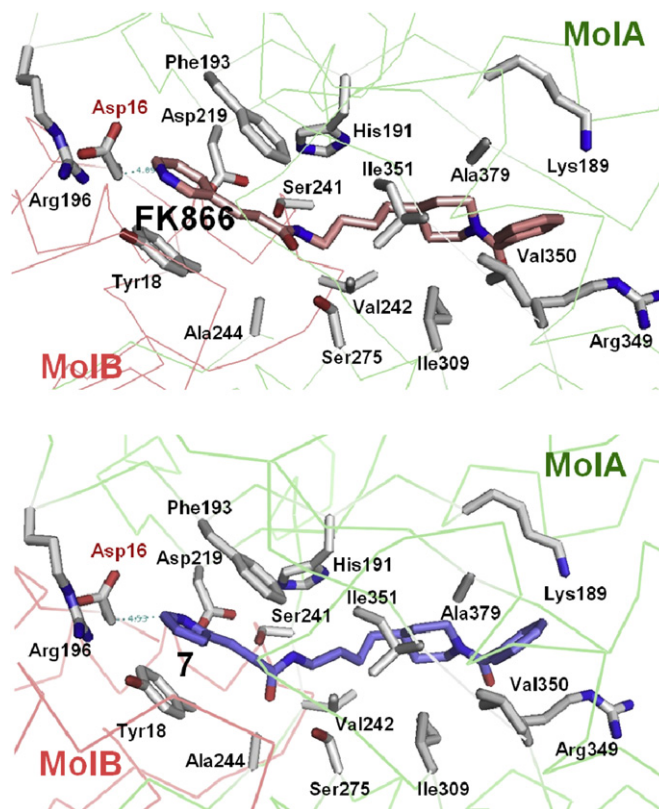


**Fig. 6.** Modes of binding of FK866 and 7 with NAMPTase. Both inhibitors were shown in pink (FK866) and blue (7). Red text indicates the residue in MoIB. (For interpretation of the references to color in this figure legend, the reader is referred to the web version of this article.)

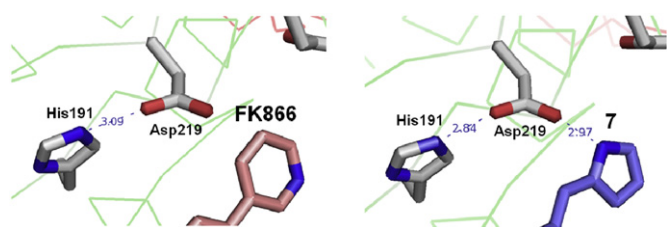


**Fig. 7.** Ionic interaction between His191(A), Asp219(A), and both inhibitors. Colors of inhibitors were same as Fig. 5. (For interpretation of the references to color in this figure legend, the reader is referred to the web version of this article.)

**Table 3**

Data collection and refinement statistics.

Data collection statistics	
Dataset	NAmPRTase-7 Complex
X-ray source	PAL-4A
Wavelength (Å)	1.0000
Space group	$P2_1$
Unit-cell dimensions (Å, °)	$a = 60.3, b = 106.5, c = 83.1, \beta = 96.5$
Resolution range (Å)	50–3.0 (3.05–3.0)
Observed reflections	83,924
Unique reflections	20,888
Completeness (%)	99.9(99.9)
$R_{\text{merge}}^a$ (%)	17.2 (39.5)
$I/\sigma$ (I)	6.1 (3.3)
Refinement statistics	
Resolution range	50–3.0
$R_{\text{work}}^b$ (%)	22.8
$R_{\text{free}}$ (%)	25.9
r.m.s.d. from ideal geometry	
r.m.s.d. bond length (Å)	0.012
r.m.s.d. bond angle (°)	1.7
Ramachandran statistics	
Most favored (%)	97.2
Additional (%)	2.8
Generously allowed (%)	0

PAL-4A, Pohang Light Source 4A HFMX beamline; r.m.s.d., root-mean-square deviation. Values in parentheses refer to the highest resolution shells.

<sup>a</sup>  $R_{\text{merge}} = \frac{\sum_h \sum_i |I(h)_i - \langle I(h) \rangle|}{\sum_h \sum_i I(h)_i}$ , where  $I(h)$  is the intensity of reflection  $h$ ,  $\Sigma_h$  is the sum over all reflections, and  $\Sigma_i$  is the sum over  $i$  measurements of reflection  $h$ .

<sup>b</sup>  $R_{\text{work}} = \frac{\sum_{hkl} ||F_o| - |F_c||}{\sum_{hkl} |F_o|}$ ; 10% of the reflections were excluded for the  $R_{\text{free}}$  calculation.

### 3. Conclusion

We have described the design and synthesis of FK866 analogs developed by modifications of the pyridine ring with various heteroaromatic rings. Among the newly synthesized compounds, compound **7** showed the most potent anti-cancer activity. The pyrrole group of **7** might be a substitution group instead of the pyridine ring to potentially achieve better metabolic stability *in vivo*, to solve the rapid metabolism of FK866 to FK866-N-oxide. Analysis of the X-ray co-crystal structures of NAmPRTase-FK866 complex and NAmPRTase-**7** complex showed that Asp219 in the active site of the enzyme could contribute to an additional ionic interaction with the pyrrole nitrogen of compound **7**. The mode of binding interactions might be applied to the strategy related to developing an anti-cancer agent based on the FK866 structure. Further investigations including binding affinity, solubility, and pharmacokinetic characteristics of FK866 and **7** are in progress.

### 4. Experimental protocols

#### 4.1. Chemistry

Starting materials, reagents, and solvents were purchased from Aldrich Chemical Co. (Milwaukee, WI) and TCI (Tokyo) and used as

supplied without further purification. Proton nuclear magnetic resonance spectroscopy was performed on a JEOL JNM-LA 300 WB and 400 WB spectrometer, and spectra were taken in  $\text{CDCl}_3$  or  $\text{DMSO}-d_6$ . Unless otherwise noted, chemical shifts are expressed as ppm downfield from tetramethylsilane as the internal standard, and  $J$  values are given in Hz. Data is reported as follows: chemical shift, multiplicity (s, singlet; d, doublet; t, triplet; m, multiplet; b, broad; app., apparent), coupling constants, and integration. Mass spectroscopy was carried out on MALDI-TOF or FAB (fast atom bombardment) instruments. [FAB source: JEOL FAB source and ion gun (Cs ion beam, 30 kV acceleration)]. High-resolution mass spectra ( $m/z$ ) were recorded on a FAB (JEOL: mass range 2600 amu, 10 kV acceleration) at Korea Basic Science Institute (Daegu).

#### 4.1.1. Methyl 4-(1-benzoylpiperidin-4-yl)butanoate (**3**)

Thionyl chloride (6.7 L, 91.6 mmol) was added to 4-piperidine butyric acid hydrochloride (**2**) (9.5 g, 45.8 mmol) in methanol (30 mL) at room temperature and the reaction mixture was stirred for 2 h. After removal of the reaction solvent, the residue was partitioned between chloroform ( $3 \times 400$  mL) and sat  $\text{NaHCO}_3$  (aq) (400 mL). The combined organic layers were dried over  $\text{MgSO}_4$ , concentrated and purified by silica gel column chromatography (chloroform:methanol = 8:1) to give ester (**3**) (7.5 g, 89%). To a solution of esterified product (7.5 g, 40.5 mmol) in DCM was added pyridine (6.5 L, 81.0 mmol) and benzoyl chloride (9.4 L, 81.0 mmol). After the mixture was stirred for 3 h at room temperature, it was partitioned between DCM ( $2 \times 350$  mL) and  $\text{NH}_4\text{Cl}$  (aq) (400 mL). The combined organic layers were dried over  $\text{MgSO}_4$  and concentrated. The crude residue was purified by silica gel column chromatography (hexane:ethylacetate = 3:1) to give **3** (7.9 g). Yield: 68%;  $^1\text{H}$  NMR (300 MHz,  $\text{CDCl}_3$ )  $\delta$  (ppm) 7.35 (s, 5H), 4.71 (m, 1H), 3.68 (s, 3H), 3.63 (m, 1H), 2.98 (m, 2H), 2.34 (t,  $J = 7.5$  Hz, 2H), 1.78–1.15 (m, 9H); ESI [ $M + H$ ] = 290.5.

#### 4.1.2. (4-(4-aminobutyl)piperidin-1-yl)(phenyl)methanone (**4**)

**3** (7.8 g, 27.0 mmol) was added to LAH (1.0 g, 27.0 mmol) in THF (30 mL) and the resulting solution was stirred for 2 h at room temperature. The reaction mixture was partitioned between chloroform ( $2 \times 400$  mL) and  $\text{NH}_4\text{Cl}$  (aq) (500 mL). The combined organic layers were dried over  $\text{MgSO}_4$ , concentrated and purified by silica gel column chromatography (hexane:ethylacetate = 1:1) to give alcohol (4.6 g). Yield: 65%;  $^1\text{H}$  NMR (300 MHz,  $\text{CDCl}_3$ )  $\delta$  (ppm) 7.35 (s, 5H), 4.07 (t,  $J = 6.9$  Hz, 2H), 3.50 (s, 2H), 2.90 (d,  $J = 10.5$  Hz, 2H), 1.65–1.23 (m, 11H); ESI [ $M + H$ ] = 262.3. To a solution of alcohol (4.6 g, 17.6 mmol) in DCM (100 mL) methanesulfonyl chloride (3.0 g, 26.4 mmol) and TEA (4.9 L, 35.2 mmol) were added and the resulting solution was stirred for 2 h at room temperature. The reaction mixture was partitioned between chloroform ( $2 \times 400$  mL) and  $\text{NH}_4\text{Cl}$  (aq) (500 mL). The combined organic layers were dried over  $\text{MgSO}_4$  and were concentrated. Resulted residue was purified by silica gel column chromatography (hexane:ethylacetate = 1:1) to give methanesulfonyl protected compound (4.1 g, 68%). Next, potassium phthalimide (2.6 g, 14.2 mmol) was added to the obtained compound (4.0 g, 11.8 mmol) in DMF (80 mL). After the reaction mixture was stirred for 8 h at 50 °C, it was partitioned between ethyl acetate ( $2 \times 400$  mL) and water (400 mL). The combined organic layers were dried over  $\text{MgSO}_4$  and were concentrated. Reaction compound was purified by silica gel column chromatography (hexane:ethylacetate = 3:2) to give intermediate product (4.0 g, 87%). Hydrazine hydrate (1.0 g, 20.4 mmol) was added to the previous product (4.0 g, 10.2 mmol) in ethanol (100 mL) and the resulting solution was stirred for 1 day at room temperature then it was filtered. The filtrate was evaporated and purified by silica gel column chromatography (chloroform:methanol = 20:1) to give **4** (1.4 g). Yield: 52%;  $^1\text{H}$  NMR (300 MHz,  $\text{CDCl}_3$ )  $\delta$  (ppm) 7.39 (s, 5H),

4.71 (m, 1H), 3.75 (m, 1H), 2.96 (m, 1H), 2.73 (m, 3H), 1.81–1.13 (m, 11H), NH peak was not shown; ESI [M + H] = 261.5.

#### 4.1.3. General procedure for the synthesis of FK866 analogs (5–12)

EDC (2.0 equiv), HOBT (1.5 equiv), and TEA (1.5 equiv) were added to various acrylic acids (1.0 equiv) in DCM (3 mL) or DMF. Then, **4** (1.2 equiv) was added to the resulting solution and the reaction mixture was stirred for 3–5 h at room temperature. The reaction mixture was added to NaHCO<sub>3</sub> (aq) (100 mL) and extracted with ethyl acetate (2 × 100 mL). The combined organic layers were dried over MgSO<sub>4</sub> and were concentrated. Compounds **5–12** were obtained by silica gel column chromatography.

**4.1.3.1. (E)-N-(4-(1-benzoylpiperidin-3-yl)butyl)-3-(pyrimidin-5-yl)acrylamide (5).** Compound **5** (60.0 mg) was obtained from **23** (30.0 mg, 0.18 mmol). Yield: 84%; <sup>1</sup>H NMR (300 MHz, CDCl<sub>3</sub>) δ (ppm) 9.18 (s, 1H), 8.85 (s, 2H), 7.65 (d, *J* = 15.5 Hz, 1H), 7.39 (s, 5H), 6.55 (d, *J* = 15.6 Hz, 1H), 5.75 (m, 1H), 4.75 (s, 1H), 3.78 (s, 1H), 3.41 (q, *J* = 6.9 Hz, 2H), 2.96 (m, 2H), 1.41–1.08 (m, 11H); <sup>13</sup>C NMR (400 MHz, CDCl<sub>3</sub>) δ (ppm) 193.62, 186.19, 179.18, 174.92 (2C), 151.18, 147.83, 142.57, 141.76, 141.26 (2C), 139.21 (2C), 136.60, 40.81, 33.86, 31.96 (2C), 30.49, 25.83 (2C), 17.99, 10.68; ESI [M – H] = 391.2; HRMS (FAB) (C<sub>23</sub>H<sub>29</sub>N<sub>4</sub>O<sub>2</sub>): calcd 393.2291, found 393.2287.

**4.1.3.2. (E)-3-(2-aminopyrimidin-5-yl)-N-(4-(1-benzoylpiperidine-4-yl)butyl)acrylamide (6).** Compound **6** (14.5 mg) was obtained from **24** (29.5 mg, 0.18 mmol). Yield: 20%; <sup>1</sup>H NMR (300 MHz, CDCl<sub>3</sub>) δ (ppm) 8.45 (s, 2H), 7.48 (d, *J* = 15.9 Hz, 1H), 7.39 (s, 5H), 6.30 (d, *J* = 15.6 Hz, 1H), 5.58 (m, 1H), 5.24 (s, NH<sub>2</sub>, 2H), 4.70 (m, 1H), 3.74 (m, 1H), 3.41 (q, *J* = 6.9 Hz, 2H), 2.96 (m, 2H), 1.41–1.08 (m, 11H); <sup>13</sup>C NMR (400 MHz, CDCl<sub>3</sub>) δ (ppm) 193.59, 192.71, 184.41, 177.23 (2C), 151.22, 149.17, 142.51, 141.24 (2C), 139.23 (2C), 134.82, 129.11, 40.82, 33.87, 31.94 (2C), 29.97, 25.81 (2C), 17.94, 10.53; ESI [M – H] = 406.2; HRMS (FAB) (C<sub>23</sub>H<sub>30</sub>N<sub>5</sub>O<sub>2</sub>): calcd 408.2400, found 408.2398.

**4.1.3.3. (E)-N-(4-(1-benzoylpeperidin-4-yl)butyl)-3-(1H-pyrrol-2-yl)acrylamide (7).** Compound **7** (23.0 mg) was obtained from **28** (22.0 mg, 0.16 mmol). Yield: 38%; <sup>1</sup>H NMR (300 MHz, CDCl<sub>3</sub>) δ (ppm) 8.83 (s, NH of pyrrole, 1H), 7.52 (d, *J* = 15.0 Hz, 1H), 7.39 (s, 5H), 6.86 (s, 1H), 6.51 (s, 1H), 6.25 (s, 1H), 6.03 (d, *J* = 15.6 Hz, 1H), 5.56 (s, NH, 1H), 4.71 (m, 1H), 3.76 (m, 1H), 3.39 (q, *J* = 6.3 Hz, 2H), 2.96 (m, 2H), 1.56–1.04 (m, 11H); <sup>13</sup>C NMR (400 MHz, CDCl<sub>3</sub>) δ (ppm) 193.64, 189.14, 151.15, 144.35, 142.57, 141.61 (2C), 141.27, 139.22 (2C), 132.48, 123.71, 120.87, 118.84, 40.85, 33.88, 31.91 (2C), 30.19, 25.78 (2C), 18.14, 10.62; ESI [M + H] = 380.1; HRMS (FAB) (C<sub>23</sub>H<sub>30</sub>N<sub>3</sub>O<sub>2</sub>): calcd 380.2338, found 380.2336.

**4.1.3.4. (E)-N-(4-(1-benzoylpiperidin-3-yl)butyl)-3-(1H-pyrazol-4-yl)acrylamide (8).** Compound **8** (22.5 mg) was obtained from **31** (28.0 mg, 0.20 mmol). Yield: 28%; <sup>1</sup>H NMR (300 MHz, CDCl<sub>3</sub>) δ (ppm) 7.74 (s, 2H), 7.57 (d, *J* = 13.5 Hz, 1H), 7.41 (s, 5H), 6.20 (d, *J* = 15.3 Hz, 1H), 5.65 (s, NH, 1H), 4.68 (m, 1H), 3.72 (m, 1H), 3.40 (q, *J* = 7.2 Hz, 2H), 2.96 (m, 2H), 1.55–1.20 (m, 11H), NH proton of pyrazole was not shown; <sup>13</sup>C NMR (400 MHz, CDCl<sub>3</sub>) δ (ppm) 193.64, 188.42, 151.19 (2C), 147.45, 144.70, 142.54, 141.26 (2C), 139.22 (2C), 129.53, 128.38, 40.83, 34.07, 31.93 (2C), 30.19, 25.80 (2C), 18.13, 10.65; ESI [M + H] = 381.0; HRMS (FAB) (C<sub>22</sub>H<sub>29</sub>N<sub>4</sub>O<sub>2</sub>): calcd 381.2291, found 381.2293.

**4.1.3.5. (E)-N-(4-(1-benzoylpeperidin-4-yl)butyl)-3-(1H-imidazol-4-yl)acrylamide (9).** Compound **9** (85.0 mg) was obtained from uracanic acid (100.0 mg, 0.72 mmol). Yield: 31%; <sup>1</sup>H NMR (300 MHz, CDCl<sub>3</sub>) δ (ppm) 7.59 (s, 1H), 7.54 (d, *J* = 15.3 Hz, 1H), 7.39 (s, 5H), 7.15 (s, 1H), 6.54 (d, *J* = 14.7 Hz, 1H), 5.75 (s, NH, 1H), 4.69 (s, 1H), 3.78 (m, 1H), 3.39 (q, *J* = 6.6 Hz, 2H), 2.97 (m, 2H), 1.62–1.03 (m, 11H), NH

proton of imidazole was not shown; <sup>13</sup>C NMR (400 MHz, CDCl<sub>3</sub>) δ (ppm) 193.73, 189.11, 151.64, 150.89 (3C), 142.64 (2C), 141.32 (2C), 139.12 (2C), 128.78, 40.82, 34.03, 31.88 (2C), 30.10, 25.61 (2C), 17.94, 10.54; ESI [M – H] = 379.2; HRMS (FAB) (C<sub>22</sub>H<sub>29</sub>N<sub>4</sub>O<sub>2</sub>): calcd 381.2291, found 381.2288.

**4.1.3.6. (E)-N-(4-(1-benzoylpiperidin-3-yl)butyl)-4-(1H-indol-3-yl)but-2-enamide (10).** Compound **10** (417.0 mg) was obtained from trans-3-indole acrylic acid (200.0 mg, 0.53 mmol). Yield: 90%; <sup>1</sup>H NMR (300 MHz, CDCl<sub>3</sub>) δ (ppm) 8.58 (s, NH of indole, 1H), 7.91 (s, 1H), 7.89 (d, *J* = 15.6 Hz, 1H), 7.37 (s, 5H), 7.23 (m, 4H), 6.43 (d, *J* = 15.6 Hz, 1H), 5.78 (s, NH, 1H), 4.71 (m, 1H), 3.78 (m, 1H), 3.48 (q, *J* = 6.6 Hz, 2H), 2.98 (m, 2H), 1.45–1.11 (m, 11H); <sup>13</sup>C NMR (400 MHz, CDCl<sub>3</sub>) δ (ppm) 193.63, 189.71, 152.10, 151.25, 148.94, 142.50, 141.25 (2C), 141.00, 139.24 (2C), 137.40, 134.56, 132.11, 131.12, 125.86, 122.68, 120.49, 40.86, 31.95, 30.23 (2C), 25.81 (2C), 20.64, 18.30, 10.72; ESI [M – H] = 428.0; HRMS (FAB) (C<sub>27</sub>H<sub>32</sub>N<sub>3</sub>O<sub>2</sub>): calcd 430.2495, found 430.2491.

**4.1.3.7. (E)-N-(4-(1-benzoylpeperidin-4-yl)butyl)-3-(2-nitrophenyl)acrylamide (11).** Compound **11** (92.3 mg) was obtained from 2-nitrocinnamic acid (50.0 mg, 0.25 mmol). Yield: 85%; <sup>1</sup>H NMR (300 MHz, CDCl<sub>3</sub>) δ (ppm) 8.03 (d, *J* = 7.8 Hz, 1H), 7.97 (d, *J* = 15.6 Hz, 1H), 7.64 (m, 2H), 7.53 (t, *J* = 6.6 Hz, 1H), 7.39 (s, 5H), 6.34 (d, *J* = 15.6 Hz, 1H), 5.86 (s, NH, 1H), 4.73 (m, 1H), 3.75 (m, 1H), 3.42 (q, *J* = 6.9 Hz, 2H), 2.98 (m, 2H), 1.60–1.22 (m, 11H); <sup>13</sup>C NMR (400 MHz, CDCl<sub>3</sub>) δ (ppm) 193.59, 186.88, 166.08, 151.22, 150.73, 147.43, 142.91, 142.50, 141.13, 141.24 (2C), 139.22 (2C), 138.55, 136.81, 131.78, 40.76, 33.85, 31.95 (2C), 30.41, 25.80 (2C), 17.99, 10.68; ESI [M + H] = 436.0; HRMS (FAB) (C<sub>25</sub>H<sub>30</sub>N<sub>3</sub>O<sub>4</sub>): calcd 436.2236, found 436.2232.

**4.1.3.8. (E)-N-(4-(1-benzoylpeperidin-4-yl)butyl)-3-(3-nitrophenyl)acrylamide (12).** Compound **12** (94.5 mg) was obtained from 3-nitrocinnamic acid (50.0 mg, 0.25 mmol). Yield: 87%; <sup>1</sup>H NMR (300 MHz, CDCl<sub>3</sub>) δ (ppm) 8.37 (s, 1H), 8.21 (d, *J* = 8.4 Hz, 1H), 7.77 (d, *J* = 7.8 Hz, 1H), 7.69 (d, *J* = 15.6 Hz, 1H), 7.58 (t, *J* = 8.1 Hz, 1H), 7.39 (s, 5H), 6.55 (d, *J* = 15.3 Hz, 1H), 5.92 (s, NH, 1H), 4.70 (m, 1H), 3.72 (m, 1H), 3.43 (q, *J* = 6.6 Hz, 2H), 2.97 (m, 2H), 1.60–1.24 (m, 11H); <sup>13</sup>C NMR (400 MHz, CDCl<sub>3</sub>) δ (ppm) 193.60, 188.82, 166.49, 153.54, 151.57, 151.18, 148.33, 143.12, 142.53, 141.25 (2C), 139.20 (2C), 135.62, 135.42, 132.61, 40.83, 33.83, 31.95 (2C), 30.42, 25.75 (2C), 17.99, 10.67; ESI [M + H] = 436.0; HRMS (FAB) (C<sub>25</sub>H<sub>30</sub>N<sub>3</sub>O<sub>4</sub>): calcd 436.2236, found 436.2232.

#### 4.1.4. General method for N-alkylation of FK-866 analogs (14–17)

To a solution of compounds **7–10** (1.0 equiv) were added sodium hydride (3.0 equiv) in DMF. Then **13** (1.5 equiv) was added to the resulting solution. After the reaction mixture was stirred for 10–15 h at room temperature, it was partitioned between ethyl acetate (2 × 40 mL) and NaHCO<sub>3</sub> (aq) (40 mL). The combined organic layers were dried over MgSO<sub>4</sub> and were concentrated. The residues were added 1 N HCl was added in the residues dissolved THF. The solution was stirred for 2–3 h at room temperature and was partitioned between ethyl acetate (2 × 30 mL) and NaHCO<sub>3</sub> (aq) (40 mL). The combined organic layers were dried over MgSO<sub>4</sub> and were concentrated. **14–17** were obtained by silica gel column chromatography.

**4.1.4.1. (E)-N-(4-(1-benzoylpeperidin-4-yl)butyl)-3-(1-(4-hydroxy-3-(hydroxymethyl)butyl)-1H-pyrrol-2-yl)acrylamide (14).** Compound **14** (3.2 mg) was obtained from **7** (10.8 mg, 0.028 mmol). Yield: 23%; <sup>1</sup>H NMR (300 MHz, CDCl<sub>3</sub>) δ (ppm) 7.59 (d, *J* = 15.3 Hz, 1H), 7.39 (s, 5H), 6.78 (m, 1H), 6.59 (m, 1H), 6.17 (m, 1H), 6.16 (d, *J* = 15.6 Hz, 1H), 5.75 (m, NH, 1H), 4.70 (m, 1H), 4.11 (m, 2H), 3.85 (m, 2H), 3.75 (m,

2H), 3.39 (q,  $J = 6.0$  Hz, 2H), 2.97 (m, 3H), 1.84 (m, 3H), 1.57–1.15 (m, 11H);  $^{13}\text{C}$  NMR (400 MHz,  $\text{CDCl}_3$ )  $\delta$  (ppm) 194.65, 185.97, 151.86, 145.72, 143.01, 141.25 (2C), 140.44, 139.28 (2C), 133.97, 131.98, 131.10, 123.10, 61.69 (2C), 43.54, 40.48, 38.25, 34.68, 28.63(2C), 26.75, 25.11 (2C), 17.89, 16.70, 10.88; ESI [M + H] = 482.0; HRMS (FAB) ( $\text{C}_{28}\text{H}_{40}\text{N}_3\text{O}_4$ ): calcd 482.3019, found 482.3017.

4.1.4.2. (*E*)-*N*-(4-(1-benzoylpeperidin-4-yl)butyl)-3-(1-(4-hydroxy-3-(hydroxymethyl)butyl)-1*H*-pyrazol-4-yl)acrylamide (**15**). Compound **15** (5.0 mg) was obtained from **8** (20.0 mg, 0.05 mmol). Yield: 20%;  $^1\text{H}$  NMR (300 MHz,  $\text{CDCl}_3$ )  $\delta$  (ppm) 7.65 (s, 1H), 7.54 (s, 1H), 7.49 (d,  $J = 15.9$  Hz, 1H), 7.39 (s, 5H), 6.15 (d,  $J = 15.6$  Hz, 1H), 5.71 (s, NH, 1H), 4.70 (m, 1H), 4.24 (t,  $J = 6.9$  Hz, 2H), 3.77 (m, 2H), 3.70 (m, 2H), 3.39 (q,  $J = 6.9$  Hz, 2H), 2.97 (m, 3H), 1.99 (m, 2H), 1.79 (m, 1H), 1.57–1.12 (m, 11H);  $^{13}\text{C}$  NMR (400 MHz,  $\text{CDCl}_3$ )  $\delta$  (ppm) 193.61, 188.41, 153.29, 151.22, 149.34, 147.78, 144.73, 142.52, 141.26 (2C), 139.24 (2C), 128.79, 61.59 (2C), 43.58, 40.81, 31.96, 30.24 (2C), 25.81 (2C), 18.13 (2C), 16.27 (2C), 10.63; ESI [M + H] = 483.2; HRMS (FAB) ( $\text{C}_{27}\text{H}_{39}\text{N}_4\text{O}_4$ ): calcd 483.2971, found 483.2968.

4.1.4.3. (*E*)-*N*-(4-(1-benzoylpiperidin-4-yl)butyl)-3-(1-(4-hydroxy-3-(hydroxymethyl)butyl)-1*H*-imidazol-4-yl)acrylamide (**16**). Compound **16** (5.0 mg) was obtained from **9** (20.0 mg, 0.05 mmol). Yield: 31%;  $^1\text{H}$  NMR (300 MHz,  $\text{CDCl}_3$ )  $\delta$  (ppm) 7.43 (s, 2H), 7.39 (s, 5H), 7.04 (s, 1H), 6.56 (d,  $J = 15.3$  Hz, 1H), 6.11 (s, NH, 1H), 4.69 (m, 1H), 4.04 (m, 2H), 3.78 (m, 5H), 3.38 (q,  $J = 6.3$  Hz, 2H), 3.01 (m, 2H), 2.04 (m, 1H), 1.92 (m, 2H), 1.60–1.11 (m, 11H);  $^{13}\text{C}$  NMR (400 MHz,  $\text{CDCl}_3$ )  $\delta$  (ppm) 193.62, 185.29, 153.31, 151.25, 149.15, 145.71, 142.50, 141.25 (2C), 139.25 (2C), 131.79, 129.19, 62.10 (2C), 37.46, 32.64, 30.09, 29.82 (2C), 25.78 (2C), 25.71, 20.30, 18.01, 17.64, 10.58; ESI [M + H] = 483.4; HRMS (FAB) ( $\text{C}_{27}\text{H}_{39}\text{N}_4\text{O}_4$ ): calcd 483.2971, found 483.2970.

4.1.4.4. (*E*)-*N*-(4-(1-benzoylpeperidin-4-yl)butyl)-3-(1-(4-hydroxy-3-(hydroxymethyl)butyl)-1*H*-indol-3-yl)acrylamide (**17**). Compound **17** (28.0 mg) was obtained from **10** (96.0 mg, 1.86 mmol). Yield: 12%;  $^1\text{H}$  NMR (300 MHz,  $\text{CDCl}_3$ )  $\delta$  (ppm) 7.89 (d,  $J = 7.8$  Hz, 1H), 7.83 (d,  $J = 15.6$  Hz, 1H), 7.37 (s, 5H), 7.35 (m, 2H), 7.24 (m, 2H), 6.42 (d,  $J = 15.3$  Hz, 1H), 5.83 (s, NH, 1H), 4.63 (m, 1H), 4.20 (m, 2H), 3.77 (m, 5H), 3.41 (q,  $J = 6.6$  Hz, 2H), 2.94 (m, 2H), 1.95 (m, 2H), 1.81 (m, 1H), 1.57–1.26 (m, 11H);  $^{13}\text{C}$  NMR (400 MHz,  $\text{CDCl}_3$ )  $\delta$  (ppm) 193.63, 190.22, 152.19, 151.08, 148.55, 145.20, 142.54, 141.24 (2C), 139.18 (2C), 138.39, 134.06, 131.81, 131.34, 124.93, 120.84, 118.38, 61.53 (2C), 40.82, 36.39, 34.03, 31.88 (3C), 30.18, 25.69 (2C), 18.13, 15.98, 10.64; ESI [M + H] = 532.0; HRMS (FAB) ( $\text{C}_{32}\text{H}_{42}\text{N}_3\text{O}_4$ ): calcd 532.3725, found 532.3177.

4.1.5. (*E*)-*N*-(4-(1-benzoylpeperidin-4-yl)butyl)-3-(1-methyl-1*H*-pyrrol-2-yl)acrylamide (**18**)

To a solution of **7** (8.0 mg, 0.02 mmol) was added sodium hydride (1.4 mg, 0.06 mmol) and methyl iodide (2.5  $\mu\text{l}$ , 0.04 mmol) in DMF. The reaction mixture was stirred for 9 h at 55 °C and it was partitioned between ethyl acetate (2  $\times$  20 mL) and  $\text{NH}_4\text{Cl}$  (aq) (20 mL). The combined organic layers were dried over  $\text{MgSO}_4$  and were concentrated. The residue was obtained by silica gel column chromatography (chloroform:methanol = 80:1) to give **18** (2.3 mg). Yield: 29%;  $^1\text{H}$  NMR (300 MHz,  $\text{CDCl}_3$ )  $\delta$  (ppm) 7.59 (d,  $J = 15.0$  Hz, 1H), 7.39 (s, 5H), 6.71 (m, 1H), 6.58 (m, 1H), 6.16 (m, 1H), 6.12 (d,  $J = 15.0$  Hz, 1H), 5.47 (s, NH, 1H), 4.71 (m, 1H), 3.70 (s, 3H), 3.62 (m, 1H), 3.40 (q,  $J = 6.6$  Hz, 2H), 2.97 (m, 2H), 1.44–1.10 (m, 11H);  $^{13}\text{C}$  NMR (400 MHz,  $\text{CDCl}_3$ )  $\delta$  (ppm) 193.60, 186.40, 151.27, 144.03, 142.49, 141.92, 141.25 (2C), 139.25 (2C), 138.15, 128.72, 127.31, 116.91, 40.84, 33.24, 30.23 (2C), 29.03, 26.50, 25.84 (2C), 18.23, 10.70; ESI [M + H] = 394.1; HRMS (FAB) ( $\text{C}_{24}\text{H}_{32}\text{N}_3\text{O}_2$ ): calcd 394.2495, found 394.2491.

4.1.6. (*E*)-3-(2-aminophenyl)-*N*-(4-(1-benzoylpiperidin-4-yl)butyl)acrylamide (**19**)

Tin chloride (155.4 mg, 0.69 mmol) was added to **11** (30.0 mg, 0.07 mmol) in ethanol (3 mL). Reaction mixture was stirred for 1.2 h at 70 °C and evaporated for removing ethanol. Then, reaction mixture was partitioned between ethyl acetate (2  $\times$  20 mL) and  $\text{NaHCO}_3$  (aq) (20 mL). The combined organic layers were dried over  $\text{MgSO}_4$ , concentrated and purified by silica gel column chromatography (chloroform:methanol = 40:1) to give **19** (18.3 mg). Yield: 62%;  $^1\text{H}$  NMR (400 MHz,  $\text{CDCl}_3$ )  $\delta$  (ppm) 7.77 (d,  $J = 15.2$  Hz, 1H), 7.38 (s, 5H), 7.33 (d,  $J = 8.0$  Hz, 1H), 7.15 (t,  $J = 8.0$  Hz, 1H), 6.75 (t,  $J = 8.0$  Hz, 1H), 6.69 (d,  $J = 8.0$  Hz, 1H), 6.29 (d,  $J = 14.8$  Hz, 1H), 5.66 (s, NH, 1H), 4.69 (m, 1H), 3.94 (s,  $\text{NH}_2$ , 2H), 3.71 (m, 1H), 3.39 (q,  $J = 6.8$  Hz, 2H), 2.94 (m, 2H), 1.58–1.24 (m, 11H);  $^{13}\text{C}$  NMR (400 MHz,  $\text{CDCl}_3$ )  $\delta$  (ppm) 193.60, 188.32, 162.41 (2C), 151.46, 144.06, 142.50, 141.24 (2C) 140.33, 139.25 (2C), 131.78, 131.13, 129.19, 126.43, 40.85, 34.08, 31.96 (2C), 30.31, 25.84 (2C), 18.15, 10.71; ESI [M + H] = 406.1; HRMS (FAB) ( $\text{C}_{25}\text{H}_{32}\text{N}_3\text{O}_2$ ): calcd 406.2495, found 406.2497.

4.1.7. (*E*)-3-(3-aminophenyl)-*N*-(4-(1-benzoylpiperidin-4-yl)butyl)acrylamide (**20**)

Tin chloride (129.5 mg, 0.57 mmol) was added to **12** (25.0 mg, 0.06 mmol) in ethanol (3 mL). Reaction mixture was stirred for 1.2 h at 70 °C and evaporated for removing ethanol. Then, reaction mixture was partitioned between ethyl acetate (2  $\times$  20 mL) and  $\text{NaHCO}_3$  (aq) (20 mL). The combined organic layers were dried over  $\text{MgSO}_4$ , concentrated and purified by silica gel column chromatography (chloroform:methanol = 40:1) to give **20** (11.0 mg). Yield: 46%;  $^1\text{H}$  NMR (300 MHz,  $\text{CDCl}_3$ )  $\delta$  (ppm) 7.55 (d,  $J = 15.6$  Hz, 1H), 7.39 (s, 5H), 7.17 (t,  $J = 7.8$  Hz, 1H), 6.92 (d,  $J = 7.5$  Hz, 1H), 6.80 (t,  $J = 2.1$  Hz, 1H), 6.69 (d,  $J = 7.8$  Hz, 1H), 6.34 (d,  $J = 15.6$  Hz, 1H), 5.61 (s, NH, 1H), 4.72 (m, 1H), 3.73 (m,  $\text{NH}_2$  and piperidine proton, 3H), 3.41 (q,  $J = 6.9$  Hz, 2H), 2.95 (m, 2H), 1.56–1.24 (m, 11H);  $^{13}\text{C}$  NMR (400 MHz,  $\text{CDCl}_3$ )  $\delta$  (ppm) 193.60, 188.15, 164.12, 157.30, 151.27, 150.54, 142.87, 142.50, 141.25 (2C), 139.25 (2C), 131.25, 128.35, 126.33, 123.48, 44.39, 33.61, 31.98 (2C), 30.28, 25.83 (2C), 18.15, 10.70; ESI [M + H] = 406.3; HRMS (FAB) ( $\text{C}_{25}\text{H}_{32}\text{N}_3\text{O}_2$ ): calcd 406.2495, found 406.2494.

4.1.8. Procedure for the synthesis of pyrimidine acrylic acid building blocks

Methyl acrylate (**22**) (22.0 mmol), TEA (11.0 mmol), and palladium (II) acetate (1.1 mmol) were added to a solution of 5-bromopyrimidine (**21**) (5.5 mmol) in acetonitrile (10 mL). After stirring for 20 min under microwave reactor at 170 °C, the reaction mixture was filtered and worked up by adding ethyl acetate (2  $\times$  400 mL) and  $\text{NaHCO}_3$  (aq) (400 mL). The combined organic layers were dried over  $\text{MgSO}_4$  and were concentrated. Resulted compound (**27**) was obtained by silica gel column chromatography (hexane:ethylacetate = 1:1). Then this product was stirred in 5% sodium hydroxide in 20% water in methanol (5 mL) for 2 h at room temperature. The reaction mixture was quenched by careful addition of 1 N HCl to neutralize. After remove the solvent, the remaining residues are dissolved with chloroform:methanol = 5:1 and filtered. The filtrate was evaporated and purified by silica gel column chromatography to give **23–24**.

4.1.8.1. (*E*)-3-(pyrimidin-5-yl)acrylic acid (**23**). Compound **23** (59.0 mg) was obtained from **21a** (356.5 mg, 2.24 mmol). Yield: 18%;  $^1\text{H}$  NMR (300 MHz,  $\text{CDCl}_3$ )  $\delta$  (ppm) 9.17 (s, 1H), 8.89 (s, 2H), 7.65 (d,  $J = 16.4$  Hz, 1H), 6.62 (d,  $J = 16.2$  Hz, 1H); ESI [M – H] = 148.9.

4.1.8.2. (*E*)-3-(2-aminopyrimidin-5-yl)acrylic acid (**24**). Compound **24** (29.5 mg) was obtained from **21b** (180.0 mg, 1.03 mmol). Yield:

17%;  $^1\text{H}$  NMR (300 MHz,  $\text{CDCl}_3$ )  $\delta$  (ppm) 8.52 (s, 2H), 7.51 (d,  $J = 16.5$  Hz, 1H), 6.38 (d,  $J = 16.5$  Hz, 1H), 5.54 (s, NH2, 2H); ESI  $[\text{M} - \text{H}] = 164.0$ .

#### 4.1.9. *tert*-butyl 1*H*-pyrrole-1-carboxylate (**26**)

$\text{Boc}_2\text{O}$  (9.8 g, 44.7 mmol) and TEA (6.3 mL, 44.7 mmol) was added to pyrrole (**25**) (3.0 g, 29.8 mmol) in DCM (15 mL) and the resulting mixture was stirred for 2 h at room temperature and then worked up with DCM ( $2 \times 400$  mL) and water (400 mL). The combined organic layers were dried over  $\text{MgSO}_4$  and were concentrated to obtain **26** as white solid (7.5 g). Yield: 94%;  $^1\text{H}$  NMR (300 MHz,  $\text{CDCl}_3$ )  $\delta$  (ppm) 7.26 (s, 2H), 7.24 (t,  $J = 2.4$  Hz, 1H), 6.22 (t,  $J = 2.4$  Hz, 1H), 1.60 (d,  $J = 11.7$  Hz, 9H); ESI  $[\text{M} + \text{H}] = 169.0$ .

#### 4.1.10. (*E*)-*tert*-butyl 2-(3-methoxy-3-oxoprop-1-enyl)-1*H*-pyrrole-1-carboxylate (**27**)

Palladium (II) acetate (1.0 g, 4.5 mmol) was added to a solution of methyl acrylate (**22**) (2.0 mL, 22.4 mmol) and **26** (7.5 g, 44.8 mmol) in acetic acid, dioxane, and DMSO (3:9:1, 30 mL). The resulting mixture was stirred at 35 °C for 96 h in a flask left open to the atmosphere. The reaction mixture was diluted with diethyl ether (100 mL) and water (20 mL). The reaction mixture was filtered through a plug of celite. The combined organic layers were dried over  $\text{MgSO}_4$ , concentrated and purified by silica gel column chromatography (hexane:ethylacetate = 30:1) to give **27** (2.5 g). Yield: 23%;  $^1\text{H}$  NMR (300 MHz,  $\text{CDCl}_3$ )  $\delta$  (ppm) 8.33 (d,  $J = 16.2$  Hz, 1H), 7.40 (q,  $J = 1.5$  Hz, 1H), 6.71 (t,  $J = 1.8$  Hz, 1H), 6.23 (d,  $J = 15.9$  Hz, 1H), 6.22 (t,  $J = 3.3$  Hz, 1H), 3.78 (s, 3H), 1.63 (s, 9H); ESI  $[\text{M} - \text{H}] = 250.0$ .

#### 4.1.11. (*E*)-3-(1*H*-pyrrol-2-yl) acrylic acid (**28**)

After **27** (100.0 mg, 0.4 mmol) was stirred with TFA in DCM (3 mL) for 1 h at room temperature, the reaction mixture was worked up with DCM ( $2 \times 40$  mL) and  $\text{NaHCO}_3$  (aq) (40 mL). The combined organic layers were dried over  $\text{MgSO}_4$  and were concentrated. Resulted residue was purified by silica gel chromatography (chloroform:methanol = 50:1). Next, the obtained compound (45.3 mg, 75%) was stirred with 5% NaOH in methanol (2 mL) for 4 h at room temperature. The reaction mixture was neutralized by 1 N HCl. After evaporation neutralized water, the residue was dissolved with chloroform:methanol = 5:1 and purified silica gel column chromatography (chloroform:methanol = 30:1) to give **28** (25 mg). Yield: 91%;  $^1\text{H}$  NMR (300 MHz,  $\text{CDCl}_3$ )  $\delta$  (ppm) 10.29 (s, NH, 1H), 6.15 (d,  $J = 15.9$  Hz, 1H), 5.76 (s, 1H), 5.26 (s, 1H), 4.97 (d,  $J = 16.2$  Hz, 1H), 4.94 (m, 1H); ESI  $[\text{M} + \text{H}] = 138.0$ .

#### 4.1.12. 4-Bromop-1-tosyl-1*H*-pyrazole (**30**)

TEA (380.0  $\mu\text{L}$ , 2.72 mmol) was added to 4-bromo pyrazole (**29**) (200.0 mg, 1.36 mmol) in DCM. Then, *p*-toluene sulfonyl chloride (260.0 mg, 1.36 mmol) was added to the reaction mixture. After the reaction mixture was stirred for 3 h at room temperature, it was partitioned between ethyl acetate ( $2 \times 40$  mL) and  $\text{NaHCO}_3$  (aq) (40 mL). The combined organic layers were dried over  $\text{MgSO}_4$  and were concentrated. It was purified by silica gel column chromatography (hexane:ethylacetate = 25:1) to give **30** (290.0 mg). Yield: 73%;  $^1\text{H}$  NMR (300 MHz,  $\text{CDCl}_3$ )  $\delta$  (ppm) 8.11 (s, 1H), 7.91 (d,  $J = 8.4$  Hz, 2H), 7.65 (s, 1H), 7.37 (d,  $J = 7.8$  Hz, 2H), 2.44 (s, 3H); ESI  $[\text{M} + \text{H}] = 302.8$ .

#### 4.1.13. (*E*)-3-(1*H*-pyrazol-4-yl) acrylic acid (**31**)

To a solution of **30** (200.0 mg, 0.66 mmol) in DMF was added methyl acrylate (**22**) (297.4  $\mu\text{L}$ , 3.30 mmol), TEA (184.0  $\mu\text{L}$ , 1.32 mmol), palladium (II) acetate (29.6 mg, 0.13 mmol), LiCl (28.0 mg, 0.66 mmol), and tri-*ortho*-tolyl phosphine (200.9 mg, 0.66 mmol). After the reaction mixture was stirred for overnight at 140 °C it was partitioned between ethyl acetate ( $2 \times 40$  mL) and

$\text{NaHCO}_3$  (aq) (40 mL). The combined organic layers were dried over  $\text{MgSO}_4$ , concentrated and purified by silica gel chromatography (hexane:ethylacetate = 5:1, 38.2 mg, 38%). The purified compound (38.0 mg, 0.25 mmol) was stirred with 5% sodium hydroxide in methanol (2 mL) for 4 h at room temperature. The reaction mixture was neutralized by 1 N HCl. After removal of neutralized water, the residue was dissolved with chloroform:methanol 5:1 and stirred for a while. The reaction mixture was evaporated and purified by silica gel column chromatography (hexane:ethylacetate = 4:1) to give **31** (28.0 mg). Yield: 78%;  $^1\text{H}$  NMR (300 MHz,  $\text{DMSO}-d_6$ )  $\delta$  (ppm) 8.66 (s, NH, 1H), 8.03 (s, 2H), 7.52 (d,  $J = 15.9$  Hz, 1H), 6.24 (d,  $J = 15.9$  Hz, 1H); ESI  $[\text{M} - \text{H}] = 137.9$ .

#### 4.1.14. 2-(Hydroxymethyl) butane-1,4-diol (**33**)

To a reflux solution of triethyl 1,1,2-ethane tricarboxylate (**32**) (5.0 g, 20.3 mmol) and sodium borohydride (2.3 g, 60.9 mmol) in *tert*-butyl alcohol (40 mL), methanol (2.5 mL) was added in the reaction mixture in three aliquots over 0.5 h. The resulting solution was heated under reflux condition for additional 0.5 h and allowed to cool down to room temperature. 1 N HCl was added with care until the solution was neutral. The solution was filtered and filtrate was extracted with ethanol. The residue was purified by silica gel column chromatography (chloroform:methanol = 7:1) to give **33** (2.1 g). Yield: 88%;  $^1\text{H}$  NMR (300 MHz,  $\text{CDCl}_3$ )  $\delta$  (ppm) 3.80 (m, 6H), 1.93 (q,  $J = 5.4$  Hz, 1H), 1.71 (m, 2H); ESI  $[\text{M} + \text{H}] = 121.3$ .

#### 4.1.15. 2-(2,2-dimethyl-1,3-dioxan-5-yl) ethanol (**34**)

2,2-Dimethoxy propane (2.5 mL, 20 mmol) and *p*-toluene sulfonic acid monohydrate (180.0 mg, 0.9 mmol) were added to a solution of **33** (2.1 g, 17.9 mmol) in THF (10 mL). The resulting solution was stirred for 4 h at room temperature. The reaction mixture was neutralized by addition of TEA. The solvent was removed and the residue was purified by silica gel column chromatography (hexane:ethylacetate = 4:1) to give **34** (1.7 g). Yield: 59%;  $^1\text{H}$  NMR (300 MHz,  $\text{CDCl}_3$ )  $\delta$  (ppm) 3.97 (m, 2H), 3.75 (m, 4H), 1.95 (m, 1H), 1.43 (s, 6H); ESI  $[\text{M} - \text{H}] = 158.0$

#### 4.1.16. 2-(2,2-dimethyl-1,3-dioxan-5-yl)ethyl 4-methylbenzenesulfonate (**13**)

*p*-Toluenesulfonyl chloride (2.4 g, 12.7 mmol) and pyridine (4.3 mL, 53.0 mmol) were added to a solution of **34** (1.7 g, 10.6 mmol) in DCM (10 mL). After the reaction mixture was stirred for 5 h at room temperature, it was partitioned between ethyl acetate ( $2 \times 150$  mL), water (50 mL) and 1 N HCl (25 mL). The combined organic layers were dried over  $\text{MgSO}_4$ , concentrated and purified by silica gel column chromatography (hexane:ethylacetate = 7:1) to give **13** (1.9 g). Yield: 58%;  $^1\text{H}$  NMR (300 MHz,  $\text{CDCl}_3$ )  $\delta$  (ppm) 7.80 (d,  $J = 6.9$  Hz, 2H), 7.37 (d,  $J = 8.1$  Hz, 2H), 4.02 (m, 2H), 3.83 (m, 3H), 3.52 (q,  $J = 5.1$  Hz, 1H), 2.62 (m, 1H), 2.46 (s, 3H), 2.04 (m, 2H), 1.57 (s, 6H); ESI  $[\text{M} - \text{H}] = 311.0$ .

## 4.2. Cell viability assay

### 4.2.1. Cell culture

MCF-7 cells were grown as suspension cultures in RPMI 1640. The adherent cell line HepG2 cells were cultured in DMEM medium. Both media were supplemented with 10% FBS (Invitrogen, Co.), and antibiotic-antimycotic (Invitrogen, Co.). All cell lines were incubated in a humidified atmosphere containing 5%  $\text{CO}_2$  at 37 °C. The adherent cells were detached from the culture flasks by removal of the growth medium and addition of 3 mL trypsin/EDTA solution (0.05% w/v trypsin, 0.016% w/v EDTA). After ~5–10 min incubation at 37 °C, when the cells had detached from the surface, trypsinization was stopped by the addition of 3 mL of DMEM medium containing 10% FBS.

#### 4.2.2. SRB assay

The cells were plated at a density of 50,000 cells per mL and well in 96-well plates and incubated with inhibitors for the time indicated. The SRB assay was carried out as described by Skehan et al. [22]. The drug incubation period of the cells was stopped by the addition of 50  $\mu$ l of ice cold TCA solution into the growth medium. After 1 h incubation in the refrigerator, the supernatant was discarded, the dishes were rinsed five times with deionized water, dried at room temperature (RT). 100  $\mu$ l of SRB solution was pipetted into each well and incubated at room temperature for 30 min. Then, the staining solution was decanted, the dishes were washed four times with 1% (v/v) acetic acid and dried again at RT. SRB stain unspecifically bound to protein was released by adding 1 mL of 10 mM Tris buffer per well and gentle shaking for 20 min. Finally the light extinction at 515 nm wavelength was read in an ELISA-reader. The mean values of four duplicated samples were calculated. These results were expressed as a percentage, relative to solvent treated control incubations, and  $IC_{50}$  values were calculated using nonlinear regression analysis (percent survival versus concentration).

#### 4.3. Overexpression and purification of human NAMPRTase

The human NAMPRTase gene was amplified by PCR using a GeneAmp PCR system 2400 thermocycler (Perkin Elmer). PCR was run in ThermoPol buffer (New England Biolabs) using NQ DNA polymerase (Anygen, Korea). The forward and reverse primers (5'-TAC CTA GGA TCC ATG AAT CCT GCG GCA GAA-3' and 5'-TGA CTC GAG CTA ATG ATG TGC TGC TTC CAG-3') were designed from the NAMPRTase nucleotide sequence in GenBank, accession no. NM005746. The amplified gene and the modified pET28a expression vector were digested using BamHI and XhoI, and then the NAMPRTase gene was ligated into expression vector and used to transform *Escherichia coli* strain BL21 (DE3). Transformed BL21 (DE3) cells were grown overnight at 37 °C in 50 mL Luria broth containing 50  $\mu$ g/mL kanamycin (Duchefa Biochemie). Cells were resuspended in 2  $\mu$ l of the same media, and grown at 37 °C to an  $OD_{600}$  of 0.6. His-tagged recombinant proteins were then induced using 0.5 mM isopropyl- $\beta$ -D-thiogalactoside (Pharmacia). After inducing for 20 h at 15 °C, cells were harvested and resuspended in lysis buffer [50 mM phosphate buffer pH 8.0, 300 mM NaCl, 5 mM imidazole, and 10% (v/v) glycerol]. The lysate was then produced with an ultrasonic processor (Sonics) and cleared by centrifugation at 14,000 g for 1 h. His-tagged NAMPRTase recombinant proteins were purified with Ni-NTA chelating agarose resin (Peptron, Korea) by washing with lysis buffer and eluting with 50 mM phosphate buffer (pH 8.0), 300 mM NaCl, 150 mM imidazole, 2 mM dithiothreitol (DTT), and 10% glycerol. After which eluted NAMPRTase proteins were further loaded onto a Superdex S200 16/60 column (GE Healthcare) equilibrated in 20 mM Hepes-NaOH (pH 7.5), 150 mM NaCl, 2 mM DTT, and 10% glycerol. Fractions containing human NAMPRTase was pooled and concentrated to 15 mg/mL.

#### 4.4. HPLC assay

HPLC was performed with LC-6AD pumps and an SPD-M10A diode array detector (Shimadzu) with a Shim-pack VP-ODS column (250 mm  $\times$  4.6 mm i.d., and 4.6  $\mu$ m particle size, Shimadzu). The NAMPRTase reaction was conducted at 37 °C for 15 min in 200  $\mu$ l of reaction buffer [50 mM Hepes-NaOH (pH 7.5), 10 mM MgCl<sub>2</sub>, 5 mM NAM, and 5 mM phosphoribosyl pyrophosphate (PRPP)] with 50 mM of the purified NAMPRTase protein. The reaction was terminated by adding 50  $\mu$ l of 1 M HClO<sub>4</sub>. Protein was then precipitated using centrifugation at 14,000 g for 20 min, and 200  $\mu$ l of the supernatant was neutralized with 16  $\mu$ l of 3 M K<sub>2</sub>CO<sub>3</sub>. After

centrifugation at 14,000 g for 1 h, 200  $\mu$ l of sample was filtered using Millex-GV (0.22  $\mu$ m, Millipore) and injected onto the column equilibrated in 50 mM phosphate buffer (pH 7.0) and initially eluted with 6 mL of this buffer. Further elution was performed with a 10 mL linear gradient to 20% (v/v) methanol and then 8 mL linear gradient to 95% methanol in the same buffer. A flow rate of 1 mL/min was performed. The products from NAMPRTase reaction were monitored by absorbance at 261 nm. NMN elutes 4.1 mL after injection, PRPP at 8.9 mL, and NAM at 13.4 mL (Fig. 3). To observe inhibitory activities, each previously synthesized inhibitor was added to reaction buffer in addition to using the same method for detection of the reaction products. Percent inhibition by each drug candidate was measured by a relative decrease of the amount of NMN, based on the peak area compared with a standard as the peak area when no inhibitor was added to reaction buffer.

#### 4.5. Crystallization

Crystallization trials were performed in a 24-well plate using the hanging-drop vapor diffusion method. NAMPRTase (10 mg/mL) was incubated with 0.4 mM compound 7 (protein/inhibitor molar ratio of 1:2) at 4 °C for 30 min before crystallization setup. Crystals of human NAMPRTase in complex with 7 were grown at 21 °C in 2  $\mu$ l of the drop containing equal volumes of protein/inhibitor solution and reservoir solution comprised of 100 mM Tris-HCl (pH 9.0), 19% (w/v) polyethylene glycol 3350, and 175 mM MgCl<sub>2</sub>. The crystals were cryo-protected by transferring to the reservoir solution supplemented with 15% (v/v) ethylene glycol and flash-frozen in liquid nitrogen for data collection.

#### 4.6. Structure determination

A complete data set up to 3.0 Å resolution was collected at 100 K at BL-4A of the Pohang Accelerator Laboratory, Korea. Data set was indexed and processed using the HKL-2000 package [23]. We found crystals of NAMPRTase in complex with 7 belonged to the  $P2_1$  space group and have the unit-cell dimensions  $a = 60.3$ ,  $b = 106.5$ ,  $c = 83.1$  Å,  $\beta = 96.5^\circ$ . Assuming one dimeric NAMPRTase molecule is contained in an asymmetric unit, the Matthews coefficient was calculated to be 2.41 Å<sup>3</sup>/Da; the estimated solvent content was thus 48.9% [24]. Initial molecular replacement calculations were carried out with MOLREP [25] using search models based on the structure of human NAMPRTase as free-form (PDB code 2E5B). Refinement of this structure was performed with REFMAC and CNS [26]; final crystallographic  $R$  value was 22.8% ( $R_{free} = 25.9\%$ ). All molecular graphics were created using PyMol [27]. The statistics for data collection and refinement were summarized in Table 3.

#### Acknowledgement

We thank Drs. Heung-Soo Lee and Yeon-Gil Kim for their kind support with X-ray data collection at BL-4A of Pohang Accelerator Laboratory (Pohang, Korea). This study was supported by a grant of the Korea Healthcare technology R&D Project, Ministry for Health, Welfare & Family Affairs, Republic of Korea (A062442 and A092006) and by a grant from the Institute of Medical System Engineering (iMSE) in the GIST, Republic of Korea.

#### References

- [1] L. Chen, R. Petrelli, K. Felczak, G. Gao, L. Bonnac, J.S. Yu, E.M. Bennett, K.W. Pankiewicz, *Current Medicinal Chemistry* 15 (2008) 650–670.
- [2] R.A. Frye, *Biochemical Biophysical Research Communications* 260 (1999) 273–279.
- [3] J.C. Am, C. Spennhauer, G. De Murcia, *BioEssays* 26 (2004) 882–893.

- [4] D. D'Amours, S. Desnoyers, I. D'Silva, G.G. Poirier, *Biochemical Journal* 342 (1999) 249–268.
- [5] M.C. Haigis, L.P. Guarente, *Genes and Development* 20 (2006) 2913–2921.
- [6] L.R. Saunders, E. Verdin, *Oncogene* 26 (2007) 5489–5504.
- [7] S. Beneke, J. Diefenbach, A. Burkle, *International Journal of Cancer* 111 (2004) 813–818.
- [8] C. Lengauer, K.W. Kinzler, B. Vogelstein, *Nature* 396 (1998) 643–649.
- [9] F. Nomura, M. Yaguchi, A. Togawa, M. Miyazaki, K. Isobe, M. Miyake, M. Noda, T. Nakai, *Journal of Gastroenterology and Hepatology* 15 (2000) 529–535.
- [10] G.J. Hageman, R.H. Stierum, *Mutation Research Fundamental and Molecular Mechanisms of Mutagenesis* 475 (2001) 45–56.
- [11] P.L. Pedersen, *Journal of Bioenergetics and Biomembranes* 39 (2007) 1–12.
- [12] S.E. Hufton, P.T. Moerkerk, R. Brandwijk, A.P. De Bruone, J.W. Arends, H.R. Hoogenboom, *FEBS Letters* 463 (1999) 77–82.
- [13] J.R. Van Beijnum, P.T.M. Moerkerk, A.J. Gerbers, A.P. De Brune, J.W. Arends, H.R. Hoogenboom, S.E. Hufton, *International Journal of Cancer* 101 (2002) 118–127.
- [14] G. Magni, A. Amici, M. Emanuelli, G. Orsomando, N. Raffaelli, S. Ruggieri, *Cellular and Molecular Life Sciences* 61 (2004) 19–34.
- [15] P. Bieganski, C. Brenner, *Cell* 117 (2004) 495–502.
- [16] M. Hasmann, I. Schemainda, *Cancer Research* 63 (2003) 7436–7442.
- [17] J.A. Khan, F. Forouhar, X. Tao, L. Tong, *Expert Opinion on Therapeutic Targets* 11 (2007) 695–705.
- [18] K. Holen, L.B. Saltz, E. Hollywood, K. Burk, A.R. Hanauske, *Investigational New Drugs* 26 (2008) 45–51.
- [19] J.A. Khan, X. Tao, L. Tong, *Nature Structural and Molecular Biology* 13 (2006) 582–588.
- [20] M.K. Kim, J.H. Lee, H. Kim, S.J. Park, S.H. Kim, G.B. Kang, Y.S. Lee, J.B. Kim, K.K. Kim, S.W. Suh, S.H. Eom, *Journal of Molecular Biology* 362 (2006) 66–77.
- [21] G.B. Kang, M.H. Bae, M.K. Kim, I. Im, Y.C. Kim, S.H. Eom, *Molecules and Cells* 27 (2009) 667–671.
- [22] P. Skehan, R. Storeng, D. Scudiero, A. Monks, J. McMahon, D. Vistica, J.T. Warren, H. Bokesch, S. Kenney, M.R. Boyd, *Journal of the National Cancer Institute* 82 (1990) 1107–1112.
- [23] Z. Otwinowski, W. Minor, *Methods in Enzymology* 276 (1997) 307–326.
- [24] B.W. Matthews, *Journal of Molecular Biology* 33 (1968) 491–497.
- [25] A. Vagin, A. Teplyakov, *Acta Crystallographica D* 56 (2000) 1622–1624.
- [26] M.D. Winn, G.N. Murshudov, M.Z. Papiz, *Methods in Enzymology* 374 (2003) 300–321.
- [27] W.L. DeLano, *The PyMOL Molecular Graphics System*. DeLano Scientific, Palo Alto, California, 2002.